AIAA SciTech Forum
23-27 January 2023, National Harbor, MD & Online
AIAA SCITECH 2023 Forum

10.2514/6.2023-0973

Topology Optimization of Stringer and Frame Locations Using Equivalent Radiated Power

Wesley Dossett[1], Adam McKenzie[2], Luke Crispo[3], and Il Yong Kim[4]
Queen's University, Kingston, Ontario, K7L 3N6, Canada

Fuselage structures transmit vibrations into the cabin and generate sound experienced by passengers and crew. However, acoustics is generally not considered during fuselage structural design. The main source of noise reduction coming from adding damping material to the fuselage. This paper proposes a methodology for incorporating acoustics optimization into the structural design of the fuselage. Equivalent radiated power was used within Altair OptiStruct as an indirect method for minimizing radiated sound power. The frames and stringers were removed from the fuselage and replaced with a 3D design space for topology optimization. Optimization results were used to determine frame and stringer locations. Standard frame and stringer cross-sections were used. The results were compared to a baseline design with standard stiffener spacing.

I. Introduction

An aircraft fuselage transmits vibrations from exterior sources and onboard machinery to the cabin space [1]. These vibrations generate noise that causes passenger discomfort and adversely affects flight crew health [2] [3]. Traditionally, the design of a fuselage is focused on structural and cost requirements, while cabin noise is often a secondary objective. As outlined by Mixson and Powell [1] and Wilby [4], the main method for noise reduction is to add damping material to the already completed fuselage structure design.

Structural-acoustic optimization techniques alter the distribution of material within a design space to passively reduce radiated noise, as summarized by Marburg [5]. There are multiple types of design optimization, including topology, size, and shape optimization, that have been applied to aerospace design with various goals [6]. A size optimization method was developed by Lamancusa to optimize for sound power, mean square velocity, and radiation efficiency, all over a frequency range [7]. Cunefare et al. minimized noise in stiffened cylinders caused by tonal excitations [8]. Luo and Gea performed topology optimization on a stiffened panel to determine optimal stiffener locations for minimizing radiated noise [9]. However, this methodology is only feasible at single frequencies or low frequency ranges. While these approaches were successful, there has been little integration of these structural-acoustic optimization methodologies into commercial design optimization software. Equivalent radiated power (ERP) is available as an objective function in Altair OptiStruct [10], and has been used as an approximation of sound power by Crispo et al. to determine skin thicknesses of a stiffened panel thickness using free-size optimization [11], and by Kim et al. using topography optimization in the design of an air conditioning enclosure [12]

The goal of this research is to optimize the structural design of an aircraft fuselage using Altair OptiStruct to improve acoustic performance. This paper presents a methodology for using ERP as an approximation for radiated sound power during topology optimization and validating the results with finite element analyses of the radiated sound power. The methodology is applied to determine optimal locations for stringers and frames within the fuselage to minimize noise over a broadband frequency range. The optimized geometries are compared to a fuselage design with standard stiffener distributions to determine the viability of using ERP to reduce radiated noise.

[1] MASc Student, Department of Mechanical and Materials Engineering.
[2] MASc Student, Department of Mechanical and Materials Engineering.
[3] PhD Candidate, Department of Mechanical and Materials Engineering.
[4] Professor, Department of Mechanical and Materials Engineering, email: kimiy@queensu.ca.

II. Methodology

A. ERP and Sound Power Calculations

ERP can be used to approximate the radiated sound power generated by a vibrating source [13]. In this approximation, the vibrating source is assumed to act as a piston using mean square vibration velocity [14]. The velocity is calculated through finite element analysis using the frequency response function of the structure. ERP calculations require significantly less computational resources required compared to a radiated sound power calculation with the following associated drawbacks [15]:

1. It assumes far-field radiation;
2. It does not account for acoustic short circuits; and
3. It does not account for the structure-fluid interaction when the fluid space is not modelled.

Altair OptiStruct calculates ERP as follows:

$$ERP = \frac{1}{2}\eta_{rad} c \rho_0 \sum_j A_j v_j^2 \tag{1}$$

where v_j and A_j are the normal velocity and area, respectively, of the j-th node summed over the entire radiated surface, c is the speed of sound, ρ_0 is the density of air, and η_{rad} is the radiation loss factor.

The radiated sound power generated at a single frequency is calculated by integrating far-field acoustic pressure over a hemispherical surface surrounding the structure. The hemisphere is meshed with a grid microphone nodes and the Rayleigh Integral equation is used to calculate acoustic pressure

$$p_{jm} = \sum_{j=1} \frac{f \rho_0 q}{r_{jm}} v_j i e^{-ikr_{jm}} \tag{2}$$

where p_{jm} is the acoustic pressure at the m-th microphone node due to the j-th vibrating source node, f is the frequency of the sound wave, q is the scaling factor, r_{jm} is the distance from the microphone node to source node, and k is the wavenumber. Altair OptiStruct calculates the sound power as

$$P_m = \sum_{j=1} \mathrm{Re}(p_j p_j^*) \tag{3}$$

where P_m is the OptiStruct output at the m-th microphone due to all source nodes, and p_j^* is the complex conjugate of p_j. The OptiStruct output is not the true radiated sound power and must be modified, outlined by Crispo et al. [11] as

$$P = \frac{1}{2\rho_0 c} \sum_m P_m^{Opti} A_m \tag{4}$$

where A_m is the area of the m-th microphone node. This additional calculation aligns the OptiStruct output with the theoretical equation for radiated sound power in milliwatts [14].

B. Curved Panel Model

An ERP optimization was performed on a 1.5 m x 1 m curved stiffened panel test case with nine “L” cross section stringers and four “C” cross section frames, shown in Fig. 1. A complete fuselage model was not used for ERP optimization, as it is too computationally resource intensive. The drawback of using a curved panel model is an unrealistic fixed boundary condition is introduced along the edge of the panel. The geometry consisted entirely of shell elements with an average size of 8 mm.

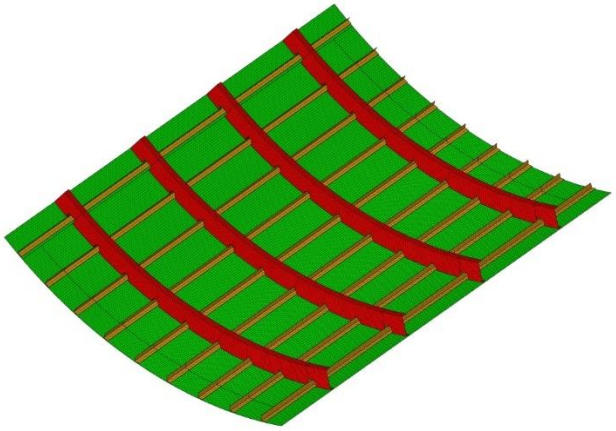

Fig. 1 Finite element model of curved panel with the baseline stiffener configuration.

Two models were developed for optimization purposes: The frame ERP optimization model in Fig. 2a) had the frames removed and replaced with a 3D hexahedral element design space, while the stringer ERP optimization model in Fig. 2b) had the stringers removed and replaced with a 3D hexahedral element design space. Thicknesses of components of the structure are listed in Table 1. All components were modelled as Aluminum 2024.

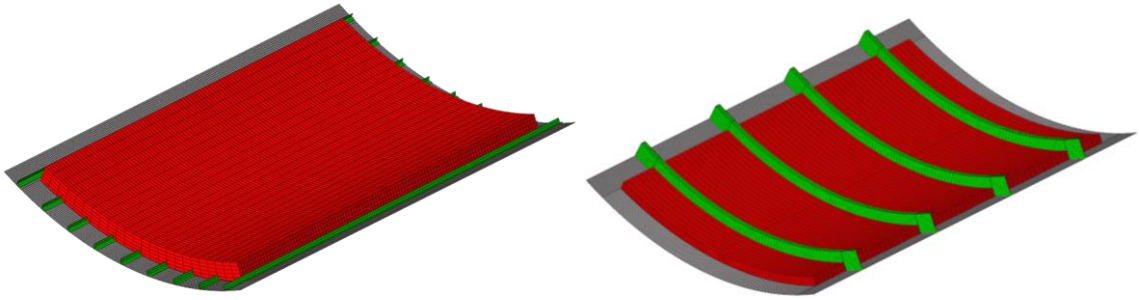

Fig. 2 Finite element models of a) frame spacing ERP optimization and b) stringer spacing ERP optimization.

Table 1 Summary of component thicknesses and material properties.

Component	Thickness [mm]	Material
Skin	2.032	Al 2024
Stringers	1.524	
Frames	0.9906	

The curved panel model was constrained with a pinned support along all four edges of the skin. An ERP optimization was performed with 25 randomly placed excitations in one quarter of the panel. Symmetry constraints were enforced during optimization to ensure that the results will have a symmetric design with only one quarter of the panel being excited.

The stiffeners were attached to the skin with rivets modelled using RBE3-CBUSH-RBE3 elements. Rivet properties were calculated using the Douglas fastener model [16], resulting in an axial stiffness of 412 kN/mm, and shear stiffness of 33 kN/mm. The hexahedral design space was connected directly to the skin using freeze contacts.

C. Fuselage Model

Sound power analysis was performed using a 4.7 m long fuselage section, shown in Fig. 3. A complete fuselage model was feasible for sound power analysis and provides higher accuracy than evaluating sound power using a curved panel model. A 1.5 m x 1 m section of the skin in the center of the fuselage was meshed with

an average element size of 8 mm. The rest of the structure was meshed with an average element size of 40 mm. Only the fine mesh region was included as radiating surfaces for the ERP and radiating sound power calculations.

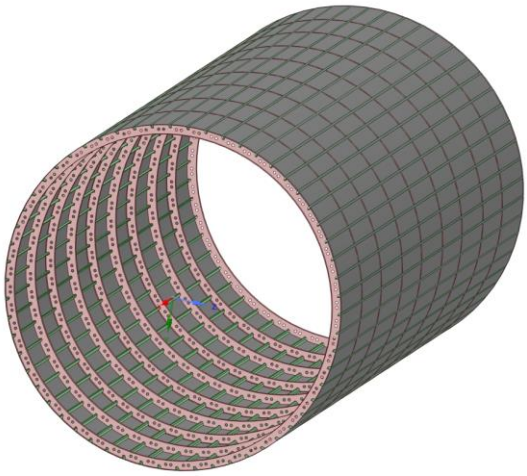

Fig. 3 Fuselage geometry used for sound power analysis.

The fuselage model was constrained with pinned supports the ends of the cylinder. There were 100 unit force excitations perpendicular to the skin each applied in separate load steps, using a rain-on-roof loading method [17]. The location of each unit load was randomly selected within the fine mesh region. The stiffeners were attached to the skin using the same method described for the curved panel model.

D. Topology Optimization

Topology optimization was used to determine the optimal distribution of material on the skin. The design variable vector, represented as $\underset{\sim}{x}$ is a vector of pseudo densities of the hexahedral elements attached to the skin. This density differs from the mass density and is used to determine the existence of material in the design. The optimization statement as shown below, minimized the sum of ERP across all skin and stiffener elements. The optimization is subject to *n* applied loads across ω frequency steps, and a mass fraction constraint. The mass fraction limit values of 0.12 and 0.10 were used for stringer optimization and frame optimization, respectively.

$$\begin{aligned} &\text{minimize:} && \sum_{n}\sum_{\omega} ERP_{\omega n}\left(\underset{\sim}{x}\right) \\ &\text{subject to:} && \underset{\sim}{M}\ddot{\underset{\sim}{u}} + \underset{\sim}{C}\dot{\underset{\sim}{u}} + \underset{\sim}{K}\underset{\sim}{u} = \underset{\sim}{f}_n e^{i\omega t} \\ & && \text{mass\_fraction} \le \text{mass\_fraction}_{\text{limit}} \\ & && 0.005 \le x_e \le 1 \\ & && \forall e \text{ skin elements}, \forall \omega \text{ frequencies}, \forall n \text{ loads} \end{aligned}$$

An extrusion constraint was applied to the density design variables such that the cross section remains constant throughout the structure. A second symmetry constraint was applied along the center plane of the model. These constraints were implemented to reduce the number of independent variables and simplify interpretation of the optimization results.

III.Results

Topology optimization was performed twice. First, the frame spacing was optimized using the model from Fig. 2a), followed by the stringer spacing optimization using the model from Fig. 2b). Each optimization result was interpreted into a fuselage model with standard "C" cross section frames and "L" cross section stringers. All models and optimizations were computed using Altair OptiStruct on a Windows PC with 16 cores @ 3.49 GHz and 64 GB RAM. Analysis run times were approximately 12 hours, with optimization times of approximately 6 hours.

A. Frame Spacing ERP Optimization

The frame spacing optimization results are shown with stringers hidden in Fig. 4. Four regions of material formed with intermediate element thicknesses. The results were interpreted into a fuselage model with alternating frame spacing, as shown in Fig. 5.

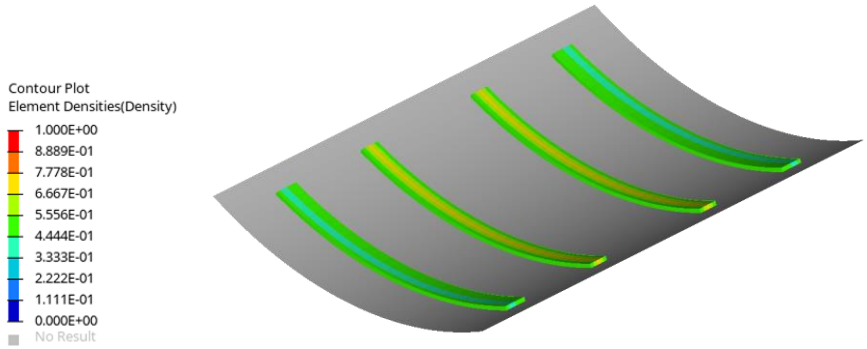

Fig. 4 Frame spacing ERP optimization results with 0.4 iso filter.

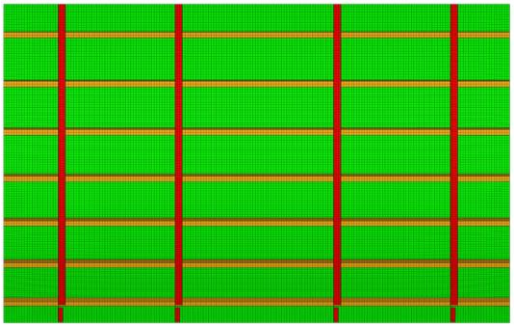

Fig. 5 Interpretation of frame spacing ERP optimization. Stringers and frames are shown in orange and red, respectively.

B. Stringer Spacing ERP Optimization

Stringer spacing ERP optimization results are shown in Fig. 6. Two wide regions of material formed with intermediate element densities. Each of these regions was interpreted as three closely packed stringers, as shown in Fig. 7.

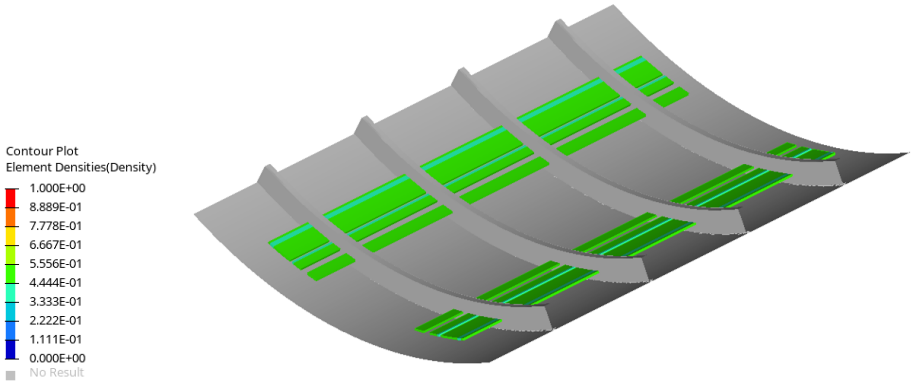

Fig. 6 Stringer spacing ERP optimization results with 0.4 iso filter.

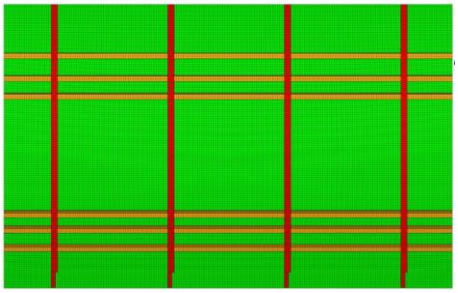

Fig. 7 Interpretation of stringer spacing ERP optimization. Stringers and frames are shown in orange and red, respectively.

C. Final Sound Power Analysis

One design interpretation was generated from each respective ERP optimization. These designs were evaluated for sound power and compared to a baseline design with constant frame and stringer spacing. The sound power and mass results are summarized in Table 2. Both new designs showed a reduced sound power compared to the baseline design. The stringer spacing model also showed a reduction in mass of 6 kg compared to the baseline design for the entire fuselage model.

Table 2 Summary of sound power analysis results.

Model	Total Sound Power [mW]	Mass [kg]
Baseline	20.6	215
Frame Optimization Interpretation	12.2	215
Stringer Optimization Interpretation	10.6	209

The frequency response of the baseline and two interpretations is shown in Fig. 8. Both interpretations show significant reductions in sound power between 600 Hz – 1000 Hz compared to the baseline design. Both interpretations also reduced sound power in frequencies below 150 Hz. However, since the magnitude of power is small compared to the response above 150 Hz, it has little significance on the total sound power. Overall, the stringer interpretation and frame interpretation reduced sound power by 48% and 41%, respectively.

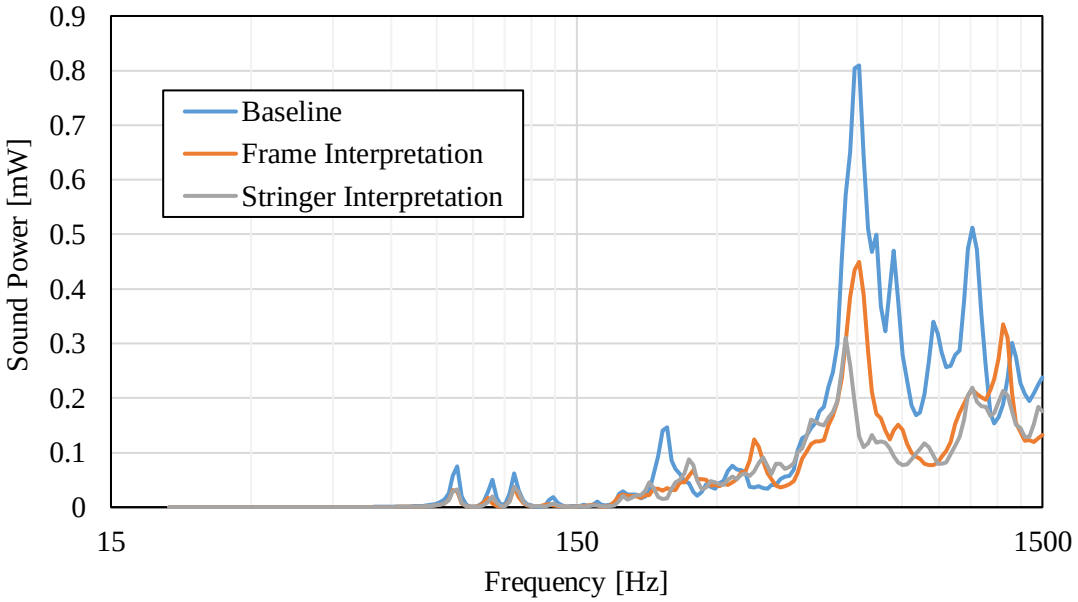

Fig. 8 Sound power results of two interpretations compared to baseline design.

A modal analysis was performed on the baseline, frame interpretation, and stringer interpretation. Modal analysis results at 600 Hz are displayed in Table 3. This frequency was chosen as it had the highest magnitude of sound power as seen in Fig. 8. The baseline design having uniform spacing between stiffeners, shows more efficiently packed mode shapes, with two or three peaks between each frame. The frame and stringer interpretations, with non-uniform spacing between stiffeners, shows less efficiently packed mode shapes. The reduction in sound power for both interpretations is likely due to the non-uniform stiffener spacing causing mode shapes to form on the skin panel less efficiently. The reduced mode shape magnitude leads to reduced vibration velocity, and ultimately reduced radiated sound.

Table 3 Modal analysis results for the baseline, frame interpretation, stringer interpretation at approximately 600 Hz.

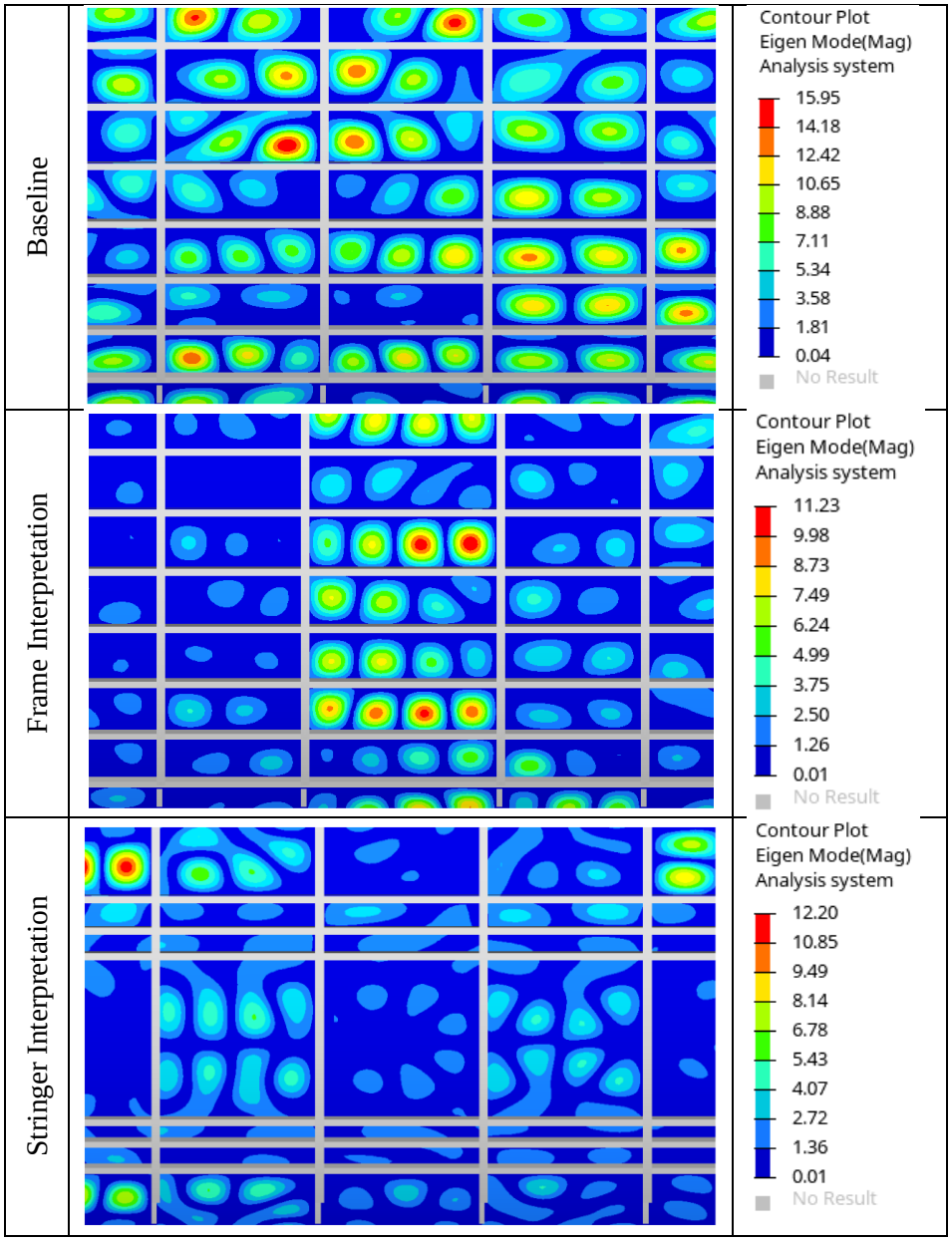

IV.Conclusion

This work presented a topology optimization methodology for minimizing ERP of an aircraft fuselage by adjusting the location of stringers and frames on a panel. ERP was used as an objective function to approximate sound power,

as sound power is not a readily available objective function in commercial FEA software. The optimization results were interpreted into two fuselage designs and compared to a standard stiffener spacing. The design interpretations with non-uniform stiffener spacing reduced the sound power by up to 48% compared to the baseline design with constant stiffener spacing. The reductions are likely due to less efficiently packed mode shapes on the skin panel with non-uniform stiffener spacing.

Future work includes considering loadcases with multiple out-of-phase excitations. The current loading considers the average response of 100 independently applied excitations. Loadcases with multiple out-of-phase excitations would be a better representation of turbulent boundary layer loading experienced by an aircraft fuselage. This study independently considered changes in stringer and frame spacing. Both optimizations resulted in reduction of sound power compared to the baseline design with equal or lighter mass. Performing concurrent optimization of both the stringer and frame spacing will increase design freedom and greater reductions in sound power would be expected. As well, other design variables of the structure such as panel thickness and stiffener cross section will be implemented into the methodology for further reductions in sound power. Small sound power reduction contributions from each design variable will compound the improvement and produce significant noise reductions.

Acknowledgments

This research was funded by the Natural Sciences and Engineering Research Council of Canada (NSERC) and by industry partner Bombardier Inc. The authors are grateful for the technical advice provided by Manuel Etchessahar, Andrew Wareing, Stephen Colavincenzo, and Sehrish Waseem from Bombardier Inc.

References

[1] Mixson, J. S., and Powell, C. A., "Review of Recent Research on Interior Noise of Propeller Aircraft," *Journal of Aircraft*, Vol. 22, No. 11, 1985, pp. 931-949. doi: 10.2514/3.45229

[2] Bouwens, J., Hiemstra-van Mastrigt, S., and Vink, P., "Ranking of Human Senses in Relation to Different In-flight Activities Contributing to the Comfort Experience of Airplane Passengers," *International Journal of Aviation Aeronautics and Aerospace*, Vol. 5, No. 2, 2018. doi: 10.15394/ijaaa.2018.1228

[3] Mellert, V., Baumann, I., Freese, N., and Weber, R., "Impact of sound and vibration on health, travel comfort and performance of flight attendants and pilots," *Aerospace Science and Technology*, Vol. 12, No. 1, Jan. 2008, pp. 18-25. doi: 10.1016/j.ast.2007.10.009

[4] Wilby, J. F., "Aircraft interior noise," *Journal of Sound and Vibration*, Vol. 190, No. 3, Feb. 1996, pp. 545-564. doi: 10.1006/jsvi.1996.0078

[5] Marburg, S., "Developments in structural-acoustic optimization for passive noise control," *Archives of Computational Methods in Engineering*, Vol. 9, No. 4, 2002, pp. 291-370. doi: 10.1007/bf03041465

[6] Zhu, J. H., Zhang, W. H., and Xia, L., "Topology Optimization in Aircraft and Aerospace Structures Design," *Archives of Computational Methods in Engineering*, Vol. 23, No. 4, Dec. 2016, pp. 595-622. doi: 10.1007/s11831-015-9151-2

[7] Lamancusa, J. S., "Numerical Optimization Techniques for Structural-Acoustic Design of Rectangular Panels," *Computers & Structures*, Vol. 48, No. 4, Aug. 1993, pp. 661-675. doi: 10.1016/0045-7949(93)90260-k

[8] Cunefare, K. A., Crane, S. P., Engelstad, S. P., and Powell, E. A., "Design minimization of noise in stiffened cylinders due to tonal external excitation," *Journal of Aircraft*, Vol. 36, No. 3, May-Jun. 1999, pp. 563-570. doi: 10.2514/2.2471

[9] Luo, J., Gea, H. C., "Optimal stiffener design for interior sound reduction using a topology optimization based approach," *J Vib Acoust*, Vol. 125, 2003, 267–273.

[10] Altair, "Altair OptiStruct 2019 User Guide," Altair Engineeering Inc., 2019.

[11] Crispo, L., Dossett, W., McKenzie, A., Kim, I. Y., "Free-Size Optimization of a Stifffened Panel Using Equivalent Radiated Power," *AIAA Aviation*, June-July 2022.

[12] Kim, H. G., Nerse, C., and Wang, S., "Topography optimization of an enclosure panel for low-frequency noise and vibration reduction using the equivalent radiated power approach," *Materials & Design*, Vol. 183, Dec. 2019. doi: 10.1016/j.matdes.2019.108125

[13] Fritze, D., Marburg, S., and Hardtke, H. J., "Estimation of Radiated Sound Power: A Case Study on Common Approximation Methods," *Acta Acustica United with Acustica*, Vol. 95, No. 5, Sep-Oct. 2009, pp. 833-842. doi: 10.3813/aaa.918214

[14] Fahy, F., and Gardonio, P., *Sound and Structural Vibration (Second Edition)*, Academic Press, Oxford, pp. 135-195

[15] Luegmair, M., and Munch, H., "Advanced Equivalent Radiated Power (ERP) Calculation for Early Vibro-Acoustic Product Optimization," *22nd International Congress on Sound and Vibration (ICSV)*, Florence, Italy, 2015.

[16] Chandregowda, S., and Reddy, G. R. C., "Evaluation of Fastener Stiffness Modelling Methods for Aircraft Structural Joints," *Advances in Mechanical Design, Materials and Manufacture*, Amer Inst Physics, India, 2018.
[17] Etchessahar, M., and Gagliardini, L., "Quantification of structural damping of a multi-layered windshield at low and medium frequencies," *The Journal of the Acoustical Society of America*, Vol. 123, No. 5, 2008, pp. 3534-3534. doi: 10.1121/1.2934499